

MATHICSE Technical Report

Nr. 26.2012

July 2012



Reduction strategies for PDE-constrained optimization problems in haemodynamics

G. Rozza, A. Manzoni, F. Negri

<http://mathicse.epfl.ch>

Address:

EPFL - SB - MATHICSE (Bâtiment MA)
Station 8 - CH-1015 - Lausanne - Switzerland

Phone: +41 21 69 37648

Fax: +41 21 69 32545

REDUCTION STRATEGIES FOR PDE-CONSTRAINED OPTIMIZATION PROBLEMS IN HAEMODYNAMICS

Gianluigi Rozza¹, Andrea Manzoni¹, and Federico Negri¹

¹ CMCS - Modelling and Scientific Computing,
MATHICSE - Mathematics Institute of Computational Science and Engineering,
EPFL - Ecole Polytechnique Fédérale de Lausanne,
Station 8, CH-1015 Lausanne, Switzerland.
e-mail: {gianluigi.rozza, andrea.manzoni, federico.negri}@epfl.ch

Keywords: inverse problems, data reconstruction, parametrized optimal control problems, reduced basis method, haemodynamics

Abstract. *Solving optimal control problems for many different scenarios obtained by varying a set of parameters in the state system is a computationally extensive task. In this paper we present a new reduced framework for the formulation, the analysis and the numerical solution of parametrized PDE-constrained optimization problems. This framework is based on a suitable saddle-point formulation of the optimal control problem and exploits the reduced basis method for the rapid and reliable solution of parametrized PDEs, leading to a relevant computational reduction with respect to traditional discretization techniques such as the finite element method. This allows a very efficient evaluation of state solutions and cost functionals, leading to an effective solution of repeated optimal control problems, even on domains of variable shape, for which a further (geometrical) reduction is pursued, relying on flexible shape parametrization techniques. This setting is applied to the solution of two problems arising from haemodynamics, dealing with both data reconstruction and data assimilation over domains of variable shape, which can be recast in a common PDE-constrained optimization formulation.*

1 INTRODUCTION

The numerical solution of PDE-constrained optimization problems such as optimal control problems usually features several computational complexities, since they require the solution of a system of partial differential equations arising from the optimality conditions – the state problem, the adjoint problem and a further set of equations ensuring the optimality of the solution. This task becomes even more challenging whenever the state system depends on a set of parameters – which can specify physical or geometrical properties of interest – and we are interested to solve a PDE-constrained optimization problem for many different scenarios, corresponding to different set of parameter values. In this case, standard techniques built over full-order discretization techniques such as the finite element method are unaffordable, featuring an overwhelming computational complexity.

Substantial computational saving becomes possible thanks to a *reduced order model* (ROM) which relies on the reduced basis (RB) method [24, 20], which allows to solve a parametrized PDE problem for any new value of the parameter set (inexpensive *Online* evaluation) once a set of (full-order) solutions have been computed for selected values of the parameter set and stored (expensive *Offline* database construction). This framework, extensively developed in the last decade and exploited in many different problems of interest, is applied for the first time in this work to the approximation of the whole PDEs system arising from the optimality conditions – thus following a *optimize-then-discretize-then-reduce* approach – rather than to the sole state problem – this latter case corresponding to a *discretize-then-reduce-then-optimize* approach [14]. In this way, the reduced basis computed during the *Offline stage* is given by a set of solutions of the optimal control problem, for selected values of the parameter set.

Computational reduction strategies such as RB methods or proper orthogonal decomposition (POD) have already been employed to speedup the solution of optimal control, as well as other PDE-constrained optimization problems, such as shape optimization and other inverse problems dealing with parametrized PDEs. First examples of optimal control problems solved by exploiting computational reduction techniques have been addressed by Ito and Ravindran, in the context either of (a preliminary version of) the reduced basis method [12] or of the proper orthogonal decomposition method. More recent contributions dealing with RB methods have been presented in both the elliptic case by Quarteroni, Rozza and Quaini [21], by Tonn, Urban and Volkwein [25], Grepl and Kärcher [6], and the parabolic case by Dedè [4]. Very recent achievements in this field have been obtained by Manzoni, Lassila, Rozza and Quarteroni [15, 14], by considering some applications of interest in haemodynamics.

The aim of this work is to apply the RB method to the class of parametrized optimal control problems featuring quadratic cost functionals and linear constraints with infinite dimensional control variable, and to develop rigorous and efficiently evaluable a posteriori error bounds for the errors in the optimal control, the state variable and the cost functional. Due to the high dimensionality of the control variable, we can not treat the control variable as a parameter itself and therefore we have to design a reduction strategy able to reduce the complexity of the whole optimal control problem simultaneously, rather than the solution of the sole state equation, in order to speed up the optimization process, as it is done for example when dealing with shape optimization problems on parametrized geometries [15, 14]. For this reason, we point out that:

- (i) in our approach the reduced scheme is built directly over the optimality conditions system rather than on the original optimization problem, following a *optimize-then-discretize-*

then-reduce approach. Indeed, we first derive the optimality system (*optimize* step), then we introduce its *truth* finite element (FE) approximation (*discretize* step) and finally we provide the RB approximation for the optimality system (*reduce* step).

- (ii) the reduced basis is made of optimal solutions of the original problem, hence the computation of each basis function requires the resolution of the FE *truth* model; moreover the reduced spaces are built for both the state, control and adjoint variables.
- (iii) to ensure the well-posedness of the RB approximation and in order to provide an *a posteriori* error estimation for the optimal control problem, we take advantage of the RB theory developed for Stokes-type problems [23], by recasting the optimality system in the framework of saddle-point problems;
- (iv) we rely on the the affine parameter dependence assumption, which provides the possibility to extract the parameter dependent components from our operators and thus exploit an Offline/Online computational procedure.

The proposed reduction strategy is then applied to a data reconstruction problem and a data assimilation problem arising in the haemodynamic contexts, the former involving a distributed optimal control problem for a Laplace problem, the latter involving a boundary control problem for a Stokes flow. In particular, the first problem we consider deals with the reconstruction, from areal data provided by eco-doppler measurements, of the blood velocity field across a two dimensional section of a carotid artery. The problem can be seen as a problem of surface reconstruction starting from scattered data, and it turns out [2] that it can be modeled as a minimization problem for a suitable PDE-penalized least-square cost functional, thus falling in our abstract formulation. The applicative nature of the problem itself suggests to consider two sets of parameters: a set of geometrical parameters, related to a suitable parametrized geometrical map describing a wide variety of shape configurations of the vessel section, and a set of parameters related to the measured data. Here we are interested in providing a reduced computational (and geometrical) framework for the real-time resolution of the reconstruction problem for different configurations of the vessel geometry and related measurements (ideally patient-specific). The second problem we deal with, inspired by the one proposed in [19], is an inverse boundary problem for the blood flow in a carotid bifurcation. Here we consider a simplified two dimensional geometry of the bifurcation and we suppose to know the inlet velocity profile and a measured velocity profile on a (one dimensional) section of the domain but not the Neumann flux on the outflow boundaries: the goal is to find the Neumann data, which will be our control variable, in order to retrieve the velocity and pressure fields on the whole domain. As in previous case, we consider both geometrical parameters, thus allowing to deal with different shape configurations, and parameters related to the measured velocity profile.

The paper is structured as follows. In Section 2 we introduce the formulation of parametrized linear-quadratic optimal control problems highlighting its saddle-point structure and introducing the related finite element approximation. In Section 3 we discuss the RB approximation and its main features. Then in Section 4 we briefly describe how to get the parametrized formulation when dealing with shape and geometrical parametrizations. Finally we apply the methodology to two data assimilation problems in haemodynamics, providing preliminary numerical results: in Section 5 we consider a surface reconstruction problem while in Section 6 we deal with an inverse boundary problem.

2 PARAMETRIZED OPTIMAL CONTROL PROBLEMS

In this section we introduce the abstract formulation of parametrized linear-quadratic optimal control problems. Let $\Omega \subset \mathbb{R}^d$ ($d = 1, 2, 3$) be an open and bounded domain with Lipschitz boundary $\Gamma = \partial\Omega$, and $\mathcal{D} \subset \mathbb{R}^p$ be a prescribed set of *input* parameters $\boldsymbol{\mu} = (\mu_1, \dots, \mu_p)$. Let \mathcal{Y}, \mathcal{U} be two Hilbert spaces for the state and control variables y and u respectively, while $\mathcal{Z} \supset \mathcal{Y}$ shall denote the observation space. Let us consider the case of a quadratic cost functional to be minimized, under the form

$$\mathcal{J}(y, u; \boldsymbol{\mu}) = \frac{1}{2}m(y - y_d(\boldsymbol{\mu}), y - y_d(\boldsymbol{\mu}); \boldsymbol{\mu}) + \frac{\alpha}{2}n(u, u; \boldsymbol{\mu}), \quad (1)$$

where $\alpha > 0$ is a given constant, $y_d(\boldsymbol{\mu}) \in \mathcal{Z}$ is a given parameter-dependent observation function, the bilinear form $m(\cdot, \cdot; \boldsymbol{\mu})$ defines the objective of the optimization while the bilinear form $n(\cdot, \cdot; \boldsymbol{\mu})$ acts as a penalization term for the control variable. Given another Hilbert space \mathcal{Q} – the adjoint space¹ – we define the linear state equation

$$\mathcal{B}(y, u, q; \boldsymbol{\mu}) = \langle G(\boldsymbol{\mu}), q \rangle \quad \forall q \in \mathcal{Q}, \quad (2)$$

where $G(\boldsymbol{\mu}) \in \mathcal{Q}'$ is a linear continuous functional acting as a forcing term and the bilinear form $\mathcal{B}(\cdot, \cdot; \boldsymbol{\mu}) : \mathcal{Y} \times \mathcal{U} \times \mathcal{Q} \rightarrow \mathbb{R}$ is given by the sum of two contributes

$$\mathcal{B}(y, u; q; \boldsymbol{\mu}) = a(y, q; \boldsymbol{\mu}) - c(u, q; \boldsymbol{\mu});$$

the bilinear form $a(\cdot, \cdot; \boldsymbol{\mu})$ represents a linear elliptic operator while the bilinear form $c(\cdot, \cdot; \boldsymbol{\mu})$ expresses the action of the control. The parametrized optimal control problem thus reads as follows: for any given $\boldsymbol{\mu} \in \mathcal{D}$,

$$\min_{y, u} \mathcal{J}(y(\boldsymbol{\mu}), u(\boldsymbol{\mu}); \boldsymbol{\mu}) \quad \text{s.t.} \quad \mathcal{B}(y(\boldsymbol{\mu}), u(\boldsymbol{\mu}), q; \boldsymbol{\mu}) = \langle G(\boldsymbol{\mu}), q \rangle, \quad \forall q \in \mathcal{Q}. \quad (3)$$

where $(y(\boldsymbol{\mu}), u(\boldsymbol{\mu})) \in \mathcal{Y} \times \mathcal{U}$. In order to ensure the well-posedness of the problem we assume the bilinear form $a(\cdot, \cdot; \boldsymbol{\mu})$ to be bounded and weakly coercive over $\mathcal{Y} \times \mathcal{Q}$, and the bilinear form $c(\cdot, \cdot; \boldsymbol{\mu})$ to be symmetric and bounded over $\mathcal{U} \times \mathcal{Q}$. Moreover we assume the bilinear form $n(\cdot, \cdot; \boldsymbol{\mu})$ to be symmetric, bounded and coercive over \mathcal{U} and the bilinear form $m(\cdot, \cdot; \boldsymbol{\mu})$ to be symmetric, bounded and positive in the norm induced by the space \mathcal{Z} .

Rather than analyzing the problem in the more usual framework of Lagrangian formalism [10] or by using Lions theory [13], it turns out to be useful in view of the application of the RB method to recast it in the framework of mixed variational problems. Let us first define the product space between the state and control space $\mathcal{X} = \mathcal{Y} \times \mathcal{U}$ and denote with $x = (y, u)$, $w = (z, v)$ its variables. We can equivalently reformulate problem (3) as: given $\boldsymbol{\mu} \in \mathcal{D}$,

$$\min_{x(\boldsymbol{\mu}) \in \mathcal{X}} \mathcal{J}(x(\boldsymbol{\mu}); \boldsymbol{\mu}) \quad \text{s.t.} \quad \mathcal{B}(x(\boldsymbol{\mu}), q; \boldsymbol{\mu}) = \langle G(\boldsymbol{\mu}), q \rangle, \quad \forall q \in \mathcal{Q}, \quad (4)$$

where the cost functional is now given by

$$\mathcal{J}(x; \boldsymbol{\mu}) = \frac{1}{2}\mathcal{A}(x, x; \boldsymbol{\mu}) - \langle F(\boldsymbol{\mu}), x \rangle, \quad (5)$$

being $\langle F(\boldsymbol{\mu}), w \rangle = m(y_d(\boldsymbol{\mu}), z) \in \mathcal{X}'$ and the bilinear form $\mathcal{A}(\cdot, \cdot; \boldsymbol{\mu})$ defined as the sum of the bilinear forms $m(\cdot, \cdot; \boldsymbol{\mu})$ and $n(\cdot, \cdot; \boldsymbol{\mu})$.

¹We shall suppose (yet without loss of generality) that state and adjoint spaces coincide, i.e. $\mathcal{Y} \equiv \mathcal{Q}$.

The constrained optimization problem (4) falls into the framework of saddle-point problems. Thanks to the hypotheses previously introduced, the assumptions of Brezzi theorem [3] can be easily verified [9] and therefore, for any $\mu \in \mathcal{D}$, the optimal control problem has a unique solution $x(\mu) \in \mathcal{X}$ that can be determined by solving the following saddle-point problem (i.e. the optimality system): given $\mu \in \mathcal{D}$, find $(x(\mu), p(\mu)) \in \mathcal{X} \times \mathcal{Q}$ such that

$$\begin{cases} \mathcal{A}(x(\mu), w; \mu) + \mathcal{B}(w, p(\mu); \mu) = \langle F(\mu), w \rangle & \forall w \in \mathcal{X}, \\ \mathcal{B}(x(\mu), q; \mu) = \langle G(\mu), q \rangle & \forall q \in \mathcal{Q}, \end{cases} \quad (6)$$

where $p(\mu)$ is the Lagrange multiplier (i.e. the adjoint variable) associated to the constraint.

2.1 Galerkin - Finite Element approximation

Let us introduce a numerical approximation of the optimality system². The standard Galerkin-FE approximation of (6) reads: given $\mu \in \mathcal{D}$, find $(x_h(\mu), p_h(\mu)) \in \mathcal{X}_h \times \mathcal{Q}_h$ such that

$$\begin{cases} \mathcal{A}(x_h(\mu), w; \mu) + \mathcal{B}(w, p_h(\mu); \mu) = \langle F(\mu), w \rangle & \forall w \in \mathcal{X}_h, \\ \mathcal{B}(x_h(\mu), q; \mu) = \langle G(\mu), q \rangle & \forall q \in \mathcal{Q}_h, \end{cases} \quad (7)$$

where $\mathcal{Y}_h \subset \mathcal{Y}$, $\mathcal{U}_h \subset \mathcal{U}$ and $\mathcal{Q}_h \subset \mathcal{Q}$ are the FE approximating spaces for the state, control and adjoint variables respectively, being $\mathcal{N} = \mathcal{N}(h)$ the dimension of the FE spaces, depending on the mesh size h . As long as the discrete spaces fulfill the discrete counterpart of the assumptions of Brezzi theorem [3], it is possible to prove the well-posedness of the FE approximation (7), see e.g. [8, 9]. At the algebraic level, we obtain the following linear system:

$$\underbrace{\begin{pmatrix} A(\mu) & B^T(\mu) \\ B(\mu) & 0 \end{pmatrix}}_{K(\mu)} \begin{pmatrix} \mathbf{x}_h(\mu) \\ \mathbf{p}_h(\mu) \end{pmatrix} = \underbrace{\begin{pmatrix} \mathbf{F}(\mu) \\ \mathbf{G}(\mu) \end{pmatrix}}_{\mathbf{b}(\mu)}, \quad (8)$$

where $\mathbf{x}_h(\mu)$ and $\mathbf{p}_h(\mu)$ denotes the vectors of the coefficients in the expansion of $x_h(\mu)$ and $p_h(\mu)$ with respect to FE basis functions. The matrix $K(\mu)$ in (8) is symmetric, indefinite, invertible for any $\mu \in \mathcal{D}$ and features a saddle-point structure where the block $B(\mu)$ contains the PDE operator acting as constraint, while the block $A(\mu)$ comes from the discretization of the functional $\mathcal{J}(\cdot; \mu)$. For the resolution of this linear system several strategies can be employed (see for instance [11, 1]): a popular alternative are the so called *reduced Hessian* methods, in which block elimination of the state and adjoint variables yield to solve a reduced system whose matrix is the Schur complement of the optimality system; an alternative strategy is given by *full space* (also called *all-at-once*) methods, where the optimality system is solved simultaneously for the state, adjoint and control variables. Both the approaches presents advantages and disadvantages and requires problem-tailored design of suitable preconditioners and iterative linear solvers; yet, beside the choice of the favorite solution algorithm, it is well known that the numerical solution of an optimal control problem entails large computational costs and may be very time-consuming already in the non-parametric case. Therefore, when performing the optimization process for many different parameter values (many-query context) or when, for a given new configuration, we want to compute the solution in a rapid way (real-time context), the computational effort may be unacceptably high and, often, unaffordable. For this reason we aim at reducing the complexity of the parametrized problem by means of suitable model order reduction techniques, yet preserving its main features and the same input-output behavior.

²We are implicitly following the *optimize-then-discretize* approach rather than the *discretize-then-optimize* approach, see e.g. [7].

3 COMPUTATIONAL REDUCTION: REDUCED BASIS METHOD

Our reduced approach to parametrized optimal control problems takes advantage of – and suitably extend – *reduced basis* (RB) methods, originally developed for rapid and reliable solutions of parametrized PDEs [24, 20]. The method is built upon (and does not replace completely) the classical FE *truth* approximating spaces of (typically very large) dimension \mathcal{N} already introduced and is based on the use of *snapshot* FE solutions of the optimal control problem, corresponding to certain parameter values, as global approximation basis functions previously computed and stored.

The reduced basis method provides an efficient way to compute an approximation $x_N(\boldsymbol{\mu})$ of $x_h(\boldsymbol{\mu})$ (and related value of the cost functional) by using a Galerkin projection on a reduced subspace made up of well-chosen FE solutions, corresponding to a specific choice $S_N = \{\boldsymbol{\mu}^1, \dots, \boldsymbol{\mu}^N\}$ of parameter values. In order to guarantee the well-posedness of the RB approximation (see [17, 18] for further details about this aggregated approach) we define the state, adjoint and control RB spaces as follows:

$$\begin{aligned}\mathcal{Y}_N &\equiv \mathcal{Q}_N = \text{span}\{y_h(\boldsymbol{\mu}^n), p_h(\boldsymbol{\mu}^n), n = 1, \dots, N\}, \\ \mathcal{U}_N &= \text{span}\{u_h(\boldsymbol{\mu}^n), n = 1, \dots, N\}.\end{aligned}$$

Moreover, let us denote $\mathcal{X}_N = \mathcal{Y}_N \times \mathcal{U}_N$. The RB approximation of (6) reads as follows: given $\boldsymbol{\mu} \in \mathcal{D}$, find $(x_N(\boldsymbol{\mu}), p_N(\boldsymbol{\mu})) \in \mathcal{X}_N \times \mathcal{Q}_N$ such that

$$\begin{cases} \mathcal{A}(x_N(\boldsymbol{\mu}), w; \boldsymbol{\mu}) + \mathcal{B}(w, p_N(\boldsymbol{\mu}); \boldsymbol{\mu}) = \langle F(\boldsymbol{\mu}), w \rangle & \forall w \in \mathcal{X}_N, \\ \mathcal{B}(x_N(\boldsymbol{\mu}), q; \boldsymbol{\mu}) = \langle G(\boldsymbol{\mu}), q \rangle & \forall q \in \mathcal{Q}_N. \end{cases} \quad (9)$$

The algebraic counterpart of the variational problem (9) is given by the following reduced linear system:

$$\underbrace{\begin{pmatrix} A_N(\boldsymbol{\mu}) & B_N^T(\boldsymbol{\mu}) \\ B_N(\boldsymbol{\mu}) & 0 \end{pmatrix}}_{K_N(\boldsymbol{\mu})} \begin{pmatrix} \mathbf{x}_N(\boldsymbol{\mu}) \\ \mathbf{p}_N(\boldsymbol{\mu}) \end{pmatrix} = \underbrace{\begin{pmatrix} \mathbf{F}_N(\boldsymbol{\mu}) \\ \mathbf{G}_N(\boldsymbol{\mu}) \end{pmatrix}}_{\mathbf{b}_N(\boldsymbol{\mu})}. \quad (10)$$

The matrix K_N is still symmetric, with saddle-point structure and, although being dense rather than sparse as in the finite element case, has dimension $5N \times 5N$, independent of the FE space dimension \mathcal{N} . Thanks to the (considerably) reduced dimension $O(N) \ll O(\mathcal{N})$ of the optimality system obtained from the RB approximation, we can provide both reliable results and rapid response in the real-time and many-query contexts.

3.1 Offline-Online strategy

While for the construction of the RB approximation spaces – and thus the optimal choice of the sample points $\boldsymbol{\mu}^n$, $1 \leq n \leq N$ – we rely on the sampling strategy based on the standard *greedy algorithm* [24, 23], to provide the standard Offline-Online computational strategy we rely on the assumption of affine parametric dependence of the bilinear and linear forms previously introduced³. In particular, assuming that the bilinear forms $a(\cdot, \cdot; \boldsymbol{\mu})$, $c(\cdot, \cdot; \boldsymbol{\mu})$, $m(\cdot, \cdot; \boldsymbol{\mu})$, $n(\cdot, \cdot; \boldsymbol{\mu})$ admit an affine decomposition implies that also the bilinear forms $\mathcal{A}(\cdot, \cdot; \boldsymbol{\mu})$ and $\mathcal{B}(\cdot, \cdot; \boldsymbol{\mu})$ can be expressed as the sum of products between given $\boldsymbol{\mu}$ -dependent functions and

³If this assumption does not hold, it could be recovered through the so-called *Empirical Interpolation Method* (EIM).

μ -independent bilinear forms. Moreover, since the affine decomposition holds also at the algebraic level, we can express the matrix $K_N(\boldsymbol{\mu})$ and the vector $\mathbf{b}_N(\boldsymbol{\mu})$ in the reduced optimality system as:

$$K_N(\boldsymbol{\mu}) = \sum_{q=1}^{Q_k} \Theta_k^q(\boldsymbol{\mu}) K_N^q, \quad \mathbf{b}_N(\boldsymbol{\mu}) = \sum_{q=1}^{Q_b} \Theta_b^q(\boldsymbol{\mu}) \mathbf{b}_N^q; \quad (11)$$

where the μ -independent matrices K_N^q and vectors \mathbf{b}_N^q represent the discrete counterparts of the corresponding bilinear and linear forms, while the μ -dependent coefficients $\Theta_*^q(\boldsymbol{\mu})$ are given functions. Therefore, thanks to the assumption of affine parametric dependence, we can decouple the formation of the matrix $K_N(\boldsymbol{\mu})$ in two stages, the Offline and Online stages, that enable the efficient resolution of the system (10) for each new parameter $\boldsymbol{\mu}$.

In particular, in the *Offline stage*, performed only once, we first compute and store the basis function and form the μ -independent matrices K_N^q , $1 \leq q \leq Q_k$ and the vectors \mathbf{b}_N^q , $1 \leq q \leq Q_b$. The operation count depends on N , Q_* and \mathcal{N} . In the *Online stage*, performed for each new value $\boldsymbol{\mu}$, we use the precomputed matrices K_N^q and vectors \mathbf{b}_N^q to assemble the (full) matrix K_N and the vector \mathbf{b}_N , and we then solve the resulting system to obtain $(\mathbf{x}_N, \mathbf{p}_N)$. The Online operation count depends on N and Q_* but is independent of \mathcal{N} .

3.2 Reliability

In the RB framework a posteriori error estimation plays a crucial role in order to guarantee the efficiency and reliability of the method. As regards efficiency the error bound is essential in the sampling procedure: the application of the estimator permits an exhaustive exploration of the parameters domain in order to select properly the basis functions. As regards reliability, at the Online stage for each new value of parameter $\boldsymbol{\mu} \in \mathcal{D}$, the a posteriori estimator permits to bound the error of the RB approximation with respect to the underlying truth approximation. Since saddle point problems are a particular case of weakly coercive (usually called *noncoercive* in the RB context) problems, the construction of an error estimator for the optimal control problems here considered can be carried out by using the Babuška stability theory. In this way we can also exploit the analogies with the RB scheme proposed to treat parametrized Stokes equations in [23]. In particular, we can provide [17, 18] a rigorous and inexpensive (i.e. \mathcal{N} -independent) a posteriori error bound $\Delta_N(\boldsymbol{\mu})$ such that

$$(\|x_h(\boldsymbol{\mu}) - x_N(\boldsymbol{\mu})\|_{\mathcal{X}}^2 + \|p_h(\boldsymbol{\mu}) - p_N(\boldsymbol{\mu})\|_{\mathcal{Q}}^2)^{1/2} \leq \Delta_N(\boldsymbol{\mu}), \quad (12)$$

where

$$\Delta_N(\boldsymbol{\mu}) = \frac{\|\mathbf{r}(\cdot; \boldsymbol{\mu})\|}{\beta_{LB}(\boldsymbol{\mu})}. \quad (13)$$

The estimator (13) is based on two ingredients: a lower bound $\beta_{LB}(\boldsymbol{\mu})$ for the Babuška inf-sup constant $\beta_h(\boldsymbol{\mu})$ of the left-hand side operator in the optimality system (7) and the dual norm of the residual of the optimality system, defined as

$$\begin{aligned} \mathbf{r}(\{w, q\}; \boldsymbol{\mu}) &= \langle F(\boldsymbol{\mu}), w \rangle - \mathcal{A}(x_N(\boldsymbol{\mu}), w; \boldsymbol{\mu}) - \mathcal{B}(w, p_N(\boldsymbol{\mu}); \boldsymbol{\mu}) \\ &\quad + \langle G(\boldsymbol{\mu}), q \rangle - \mathcal{B}(x_N(\boldsymbol{\mu}), q; \boldsymbol{\mu}), \quad \forall \{w, q\} \in \mathcal{X}_h \times \mathcal{Q}_h. \end{aligned} \quad (14)$$

Both the quantities can be computed exploiting an efficient Offline-Online strategy, thus enabling their inexpensive evaluation in the Online stage; in particular the calculation of the lower

bound $\beta_{\text{LB}}(\boldsymbol{\mu})$ can be carried out using the natural norm successive constraint method [23]. Using the same ingredients, we can also construct a rigorous and inexpensive a posteriori error bound $\Delta_N^J(\boldsymbol{\mu})$ for the error on the cost functional, i.e.

$$|\mathcal{J}(x_h(\boldsymbol{\mu}); \boldsymbol{\mu}) - \mathcal{J}(x_N(\boldsymbol{\mu}); \boldsymbol{\mu})| \leq \Delta_N^J(\boldsymbol{\mu}), \quad (15)$$

where in this case

$$\Delta_N^J(\boldsymbol{\mu}) = \frac{1}{2} \frac{\|\mathbf{r}(\cdot; \boldsymbol{\mu})\|^2}{\beta_{\text{LB}}(\boldsymbol{\mu})}. \quad (16)$$

4 PARAMETRIZED FORMULATION AND GEOMETRICAL TREATMENT

We briefly recall how the parametrized formulation (3) can be obtained, in the (less obvious) case of a geometrical parametrization; other parametrizations, involving e.g. boundary conditions or physical parameters, are in fact more direct to obtain.

Let us assume that the *original* domain $\Omega_o = \Omega_o(\boldsymbol{\mu})$ depends on a set of parameters: since the RB framework requires a reference ($\boldsymbol{\mu}$ -independent) domain Ω in order to compare, and combine, FE solutions that would be otherwise computed on different domains and grids, the original $\Omega_o(\boldsymbol{\mu})$ has to be mapped to a reference domain, in order to get the parametrized “transformed” state problem (3) – and thus the parametrized optimal control problem (2), which is the point of departure of RB approach. For the sake of the applications addressed, the construction of a parametric mapping related to geometrical properties can be managed following two different strategies [14], based on (i) patches of local *affine mappings* combined within a domain decomposition approach (see Section 6) or (ii) global nonaffine mappings (see Section 5).

Let us consider, for the sake of simplicity, a distributed control over the whole domain, and a linear elliptic state operator of order two, giving an advection-diffusion-reaction equation⁴. The “original” problem (subscript o) is as follows:

$$\min_{y_o, u_o} \mathcal{J}_o(y_o(\boldsymbol{\mu}), u_o(\boldsymbol{\mu})) \quad \text{s.t.} \quad \mathcal{B}_o(y_o(\boldsymbol{\mu}), u_o(\boldsymbol{\mu}), q) = \langle G_o(\boldsymbol{\mu}), q \rangle, \quad \forall q \in \mathcal{Q}(\Omega_o(\boldsymbol{\mu})), \quad (17)$$

with

$$\mathcal{B}_o(y_o, u_o; q_o) = a(y_o, q_o) - c(u_o, q_o),$$

where $a_o(\cdot, \cdot)$ is a linear elliptic operator and $c_o(\cdot, \cdot)$ expresses the action of the control:

$$a_o(y, q) = \sum_{k=1}^{K_{\text{dom}}} \int_{\Omega_o^k(\boldsymbol{\mu})} \left(\frac{\partial y}{\partial x_{o,i}} \nu_{ij}^{o,k}(\boldsymbol{\mu}) \frac{\partial q}{\partial x_{o,j}} + q \chi_i^{o,k}(\boldsymbol{\mu}) \frac{\partial y}{\partial x_{o,i}} + y \eta_i^{o,k}(\boldsymbol{\mu}) \frac{\partial q}{\partial x_{o,i}} + y q \right) d\Omega_o,$$

$$c_o(u, q) = \int_{\Omega_o(\boldsymbol{\mu})} u q d\Omega_o.$$

Here we consider a domain decomposition $\Omega_o(\boldsymbol{\mu}) = \cup_{k=1}^{K_{\text{dom}}} \Omega_o^k(\boldsymbol{\mu})$ consisting of mutually nonoverlapping open subdomains, such that

$$\Omega_o^k(\boldsymbol{\mu}) = T^k(\Omega^k; \boldsymbol{\mu}), \quad 1 \leq k \leq K_{\text{dom}},$$

moreover, $\boldsymbol{\nu}^{o,k} : \mathbb{R}^2 \times \mathcal{D} \rightarrow \mathbb{R}^{2 \times 2}$, $1 \leq k \leq K_{\text{dom}}$, are parametrized (symmetric positive definite) conductivity/diffusivity tensors, while $\boldsymbol{\chi}^{o,k} : \mathbb{R}^2 \times \mathcal{D} \rightarrow \mathbb{R}^2$, $\boldsymbol{\eta}^{o,k} : \mathbb{R}^2 \times \mathcal{D} \rightarrow \mathbb{R}^2$,

⁴Definition of functional spaces and differential operators follows the same notation of Section 2, but refers to the original domain $\Omega_o(\boldsymbol{\mu})$. We focus here on the differential operators appearing in the state problem, since the same procedure can be easily applied to get the transformed version of the cost functional as well.

$1 \leq k \leq K_{\text{dom}}$, are two parametrized vectors, representing transport/convective terms. By identifying $y(\boldsymbol{\mu}) = y_o(\boldsymbol{\mu}) \circ T(\cdot; \boldsymbol{\mu})$ and tracing $a_o(y, q)$ back on the reference domain Ω , it follows that the transformed bilinear form $a(\cdot, \cdot; \boldsymbol{\mu}) : X \times X \rightarrow \mathbb{R}$ can be expressed as

$$a(y, q; \boldsymbol{\mu}) = \sum_{k=1}^{K_{\text{dom}}} \int_{\Omega^k} \left(\frac{\partial y}{\partial x_i} \nu_{ij}^k(\boldsymbol{\mu}) \frac{\partial q}{\partial x_j} + y \chi_i^k(\boldsymbol{\mu}) \frac{\partial q}{\partial x_i} + y \eta_i^k(\boldsymbol{\mu}) \frac{\partial q}{\partial x_i} + y q |J_T^k(\boldsymbol{\mu})| \right) d\Omega, \quad (18)$$

where $\boldsymbol{\nu}^k(\mathbf{x}; \cdot) : \mathcal{D} \rightarrow \mathbb{R}^{2 \times 2}$, $1 \leq k \leq K_{\text{dom}}$, are parametrized tensors given by

$$\boldsymbol{\nu}^k(\mathbf{x}; \boldsymbol{\mu}) = (J_T^k(\mathbf{x}; \boldsymbol{\mu}))^{-T} \boldsymbol{\nu}^{o,k}(\boldsymbol{\mu}) (J_T^k(\mathbf{x}; \boldsymbol{\mu}))^{-1} |J_T^k(\mathbf{x}; \boldsymbol{\mu})| \quad (19)$$

where $J_T^k(\mathbf{x}; \boldsymbol{\mu}) : \mathbb{R}^2 \times \mathcal{D} \rightarrow \mathbb{R}^{2 \times 2}$ is the Jacobian matrix of the map $T^k(\cdot; \boldsymbol{\mu})$, defined as

$$(J_T^k(\mathbf{x}; \boldsymbol{\mu}))_{ij} = \frac{\partial (T^k)_i}{\partial x_j}(\mathbf{x}; \boldsymbol{\mu}) \quad (20)$$

and $|J_T^k(\mathbf{x}; \boldsymbol{\mu})| : \mathbb{R}^2 \times \mathcal{D} \rightarrow \mathbb{R}$ its determinant. In the same way, $\boldsymbol{\chi}^k(\mathbf{x}; \boldsymbol{\mu}) : \mathcal{D} \rightarrow \mathbb{R}^2$, $\boldsymbol{\eta}^k(\mathbf{x}; \boldsymbol{\mu}) : \mathcal{D} \rightarrow \mathbb{R}^2$, $1 \leq k \leq K_{\text{dom}}$, are parametrized vectors, given by

$$\boldsymbol{\chi}^k(\mathbf{x}; \boldsymbol{\mu}) = (J_T^k(\mathbf{x}; \boldsymbol{\mu}))^{-T} \boldsymbol{\chi}^{o,k}(\boldsymbol{\mu}) |J_T^k(\mathbf{x}; \boldsymbol{\mu})|, \quad \boldsymbol{\eta}^k(\mathbf{x}; \boldsymbol{\mu}) = (J_T^k(\mathbf{x}; \boldsymbol{\mu}))^{-T} \boldsymbol{\eta}^{o,k}(\boldsymbol{\mu}) |J_T^k(\mathbf{x}; \boldsymbol{\mu})|,$$

whereas

$$c(u, q; \boldsymbol{\mu}) = \sum_{k=1}^{K_{\text{dom}}} \int_{\Omega^k} u q |J_T^k(\boldsymbol{\mu})| d\Omega.$$

Hence, the original problem has been reformulated on a reference configuration, resulting in a parametrized optimal control problem where the effect of geometry variations is traced back onto its parametrized transformation tensors. *A priori*, parametrized tensors depend both on the parameter $\boldsymbol{\mu}$ and the spatial variables $\mathbf{x} \in \Omega$; however, in the affine case they depend just on the parameter components, allowing to write the affine formulation (11) by simply expanding the expression (18) in terms of the subdomains Ω^k and the different entries of the tensors. The same transformation can be operated on the quadratic cost functional or if the problem accounts for nonlinear terms.

On the other hand, if the problem is not affinely parametrized (e.g. when the geometrical transformation is not affine), the parametrized tensors in (18) depend both on the parameter $\boldsymbol{\mu}$ and the spatial coordinate \mathbf{x} . In this case, the operators can not be expressed as in (11) and we thus need an additional pre-processing, before the FE assembling stage, in order to recover the affinity assumption. According to EIM – considering for instance the tensor $\boldsymbol{\nu}^k$ – each component $\boldsymbol{\nu}_{ij}^k(\mathbf{x}, \boldsymbol{\mu})$ is approximated by an affine expression given by

$$\boldsymbol{\nu}_{ij}^k(\mathbf{x}, \boldsymbol{\mu}) = \sum_{l=1}^{K_{ijl}} \beta_l^{ijk}(\boldsymbol{\mu}) \eta_l^{ijk}(\mathbf{x}) + \varepsilon_{ij}^k(\mathbf{x}, \boldsymbol{\mu}); \quad (21)$$

all the functions β_l^{ijk} 's and η_l^{ijk} 's are efficiently computable scalar functions and the error terms are guaranteed to be under some tolerance, i.e. $\|\varepsilon_{ij}^k(\cdot; \boldsymbol{\mu})\|_\infty \leq \varepsilon_{tol}^{EIM}$, for all $\boldsymbol{\mu} \in \mathcal{D}$. In this way, we can identify the $\boldsymbol{\mu}$ -dependent functions $\beta_l^{ijk}(\boldsymbol{\mu})$ in (21) as the functions $\Theta_k^q(\boldsymbol{\mu})$ in (11), where q is a condensed index for (i, j, k, l) , while the $\boldsymbol{\mu}$ -independent functions will be treated as pre-factors in the integrals which give the $\boldsymbol{\mu}$ -independent matrices K^q .

The nonaffine treatment is really important since many problems involving more complex geometrical parametrizations and/or more complex physical properties are held by nonaffine parametric dependence.

5 APPLICATION TO A SURFACE RECONSTRUCTION PROBLEM

The first problem we consider, originally proposed in [2], deals with the reconstruction, from areal data provided by eco-dopplers measurements, of the blood velocity field in a section of a carotid artery: given a set of velocity measurements (in the horizontal direction for example) in some portions of the domains we aim at reconstructing a global velocity profile on the whole section. The problem can be seen as a problem of surface estimation starting from scattered data, with the peculiarity that the estimated surface should preserve a physiological meaning; therefore the technique employed for the reconstruction should take into account the shape of the domain and preserve the no-slip condition of the velocity field on the boundary of the domain. For this reason, the authors in [2] point out that classical surface estimation methods like thin-plate splines, tensor product splines, etc, are not well suited to tackle the problem at hand and therefore they propose to apply a smoothing technique based on the minimization of a suitable PDE-penalized least-square cost functional. Here we want to provide a flexible geometrical and computational framework enabling the rapid resolution of the problem for different shapes of the carotid sections and for different values of the observations.

Let us describe the problem at hand. We consider a domain $\Omega_o \subset \mathbb{R}^2$ (the carotid section) and we denote with $y : \Omega_o \rightarrow \mathbb{R}$ the unknown surface that we want to reconstruct starting from a given set of areal observations $\{z_i\}_{i=1}^m \subset \mathbb{R}^m$:

$$z_i = \frac{1}{|\Omega_{obs,i}^o|} \int_{\Omega_{obs,i}^o} y(\mathbf{x}) d\Omega_o,$$

being $\{\Omega_{obs,i}\}_{i=1}^n$ nonoverlapping subdomains of observation given by

$$\Omega_{obs,i}^o = \{(x_1, x_2) \mid (x_1 - x_{i,1})^2 + (x_2 - x_{i,2})^2 \leq r^2\},$$

i.e. small circles surrounding the observation points \mathbf{x}_i , see Figure 1. Since the surface we want to estimate represent the horizontal component of the blood flow in the carotid artery, thus satisfying a no-slip condition on $\partial\Omega_o$, we shall impose the variable y to vanish on the boundary, i.e. $y|_{\partial\Omega_o} = 0$. In [2, 22] the authors propose to minimize the following PDE-penalized least-square cost functional in order to recover the surface $y \in H_0^2(\Omega_o)$:

$$\min_{y \in H_0^2(\Omega_o)} J(y) = \frac{1}{2} \sum_{i=1}^m \int_{\Omega_{obs,i}^o} |y - z_i|^2 d\Omega_o + \frac{\alpha}{2} \int_{\Omega_o} (\Delta y)^2 d\Omega_o. \quad (22)$$

Problem (22) can be easily recast in the framework of linear-quadratic optimal control problems here considered by defining the control variable $u = -\Delta y$ and expressing explicitly the boundary condition satisfied by the state variable y . We end up with the following equivalent problem: given the domain Ω_o and a set of observation values $\{z_i\}_{i=1}^m$,

$$\min_{y,u} \mathcal{J}(y, u) = \frac{1}{2} \sum_{i=1}^m \int_{\Omega_{obs,i}^o} |y - z_i|^2 d\Omega_o + \frac{\alpha}{2} \int_{\Omega_o} u^2 d\Omega_o, \quad (23)$$

where $y = y(u) \in \mathcal{Y}_o$ is the solution of the following Laplace problem

$$\begin{cases} -\Delta y = u & \text{in } \Omega_o, \\ y = 0 & \text{on } \partial\Omega_o, \end{cases} \quad (24)$$

being $\mathcal{U}_o = L^2(\Omega_o)$ the control space and $\mathcal{Y}_o = H_0^1(\Omega_o)$ the space for the state variable. As already mentioned, our goal here is twofold:

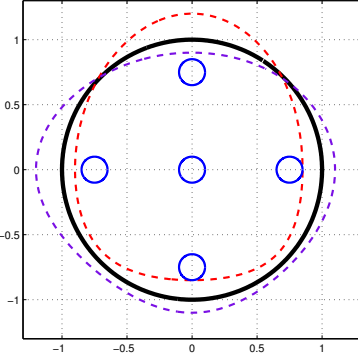


Figure 1: Reference domain $\Omega = \{(x_1, x_2) \mid x_1^2 + x_2^2 \leq 1\}$ in black, examples of *small deformations* of the reference domain in red and violet; fixed observation subdomains in blue.

- describe different configurations of the section of the carotid artery through a low dimensional shape parametrization, thus yielding a geometrical reduction;
- apply the reduced basis framework introduced above in order to provide a real-time resolution of the surface estimation problem.

5.1 Geometrical reduction

In order to achieve a strong geometrical reduction and to describe different configurations of the section of the carotid artery by using only a small number of parameters, we introduce a suitable shape parametrization based on the *free-form deformation* (FFD) technique [15]. In particular, the set of admissible shapes is defined as the set of diffeomorphic images of a

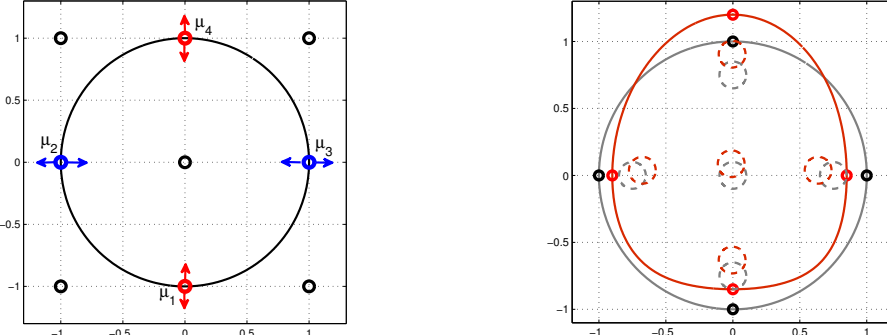


Figure 2: Schematic diagram of the FFD. On the left: reference domain Ω and FFD setting; control points depicted in red/blue can be moved in vertical/horizontal direction. On the right: in gray the reference domain Ω , in red a deformed domain $\Omega_o(\mu_g)$; black control points correspond to the reference shape (i.e. $\mu_g = 0$), while red control points correspond to the choice $\mu_g = [0.15, 0.1, -0.15, 0.2]$. The gray and red dashed circles correspond to the five observation subdomains in the reference and deformed configurations respectively.

reference domain Ω through a parametrized map $T(\mathbf{x}; \mu_g)$ depending on a set of control points acting as shape design parameters. In our case, the FFD map is built on a 3×3 lattice of control points on the rectangle $[-1, 1] \times [1, 1]$; the active control points and their allowed displacements (see Figure 2) are selected in order to describe reasonable and plausible deformations of the reference circular shape. In the end we use a parametrization with 4 design parameters μ_g

representing the vertical/horizontal displacements of selected control points; these parameters are allowed to vary in the range $[-0.15, 0.15]$, we thus define the geometrical parameters set as

$$\mathcal{D}_g = [-0.15, 0.15]^4.$$

We remark that, since the parametrized map $T(\cdot; \boldsymbol{\mu}_g) : \Omega \rightarrow \Omega_o(\boldsymbol{\mu}_g)$ is a *global* geometrical map, the observation subdomains $\Omega_{obs,i}$ are translated and deformed by action of the map itself, see Figure 2. This kind of behavior is clearly a drawback of the use of the FFD technique and it should be avoided in view of a realistic application. In fact, considering the functionality of the clinical device employed to get the measurements, i.e. the eco-doppler, it seems more reasonable to consider fixed observation subdomains. However, the employment of different shape parametrization techniques, such as those based on Radial Basis Functions (see e.g. [16]), should easily permit to overcome the problem.

We denote as a vector of input parameters also the set of observation $\{z_i\}_{i=1}^m$, i.e. we define the parameters $\mu_{obs}^i = z_i$ for $1 \leq i \leq m$ and the observation parameters space

$$\mathcal{D}_{obs} = [-0.25, 0.25]^m.$$

We finally obtain the following parametrized optimal control problem posed over the original domain $\Omega_o(\boldsymbol{\mu}_g)$: given $\boldsymbol{\mu} = (\boldsymbol{\mu}_g, \boldsymbol{\mu}_{obs}) \in \mathcal{D} = \mathcal{D}_g \times \mathcal{D}_{obs}$,

$$\min_{y,u} \mathcal{J}_o(y(\boldsymbol{\mu}), u(\boldsymbol{\mu}); \boldsymbol{\mu}_{obs}) = \frac{1}{2} \sum_{i=1}^m \int_{\Omega_{obs,i}^o(\boldsymbol{\mu})} |y(\boldsymbol{\mu}) - \mu_{obs}^i|^2 d\Omega_o + \frac{\alpha}{2} \int_{\Omega_o(\boldsymbol{\mu})} u(\boldsymbol{\mu})^2 d\Omega_o,$$

where $y(\boldsymbol{\mu}) \in \mathcal{Y}_o$ is the solution of the following state equation:

$$\begin{cases} -\Delta y(\boldsymbol{\mu}) = u(\boldsymbol{\mu}) & \text{in } \Omega_o(\boldsymbol{\mu}_g), \\ y(\boldsymbol{\mu}) = 0 & \text{on } \partial\Omega_o(\boldsymbol{\mu}_g). \end{cases}$$

Defining the adjoint space $\mathcal{Q}_o = H_0^1(\Omega_o)$ and the product space $\mathcal{X}_o = \mathcal{Y}_o \times \mathcal{Q}_o$, and introducing the weak formulation of the state equation (see Section 4), the problem can be expressed in the formulation (17): given $\boldsymbol{\mu} \in \mathcal{D}$

$$\min_{x(\boldsymbol{\mu}) \in \mathcal{X}_o} \mathcal{J}_o(x(\boldsymbol{\mu}); \boldsymbol{\mu}_{obs}) \quad \text{s.t.} \quad \mathcal{B}_o(x(\boldsymbol{\mu}), q) = 0, \quad \forall q \in \mathcal{Q}_o. \quad (25)$$

Finally, by tracing back the problem to the reference domain Ω , which is related to the original domain $\Omega_o(\boldsymbol{\mu})$ through the parametric mapping $T(\mathbf{x}; \boldsymbol{\mu})$, we obtain the parametrized formulation (3).

5.2 Numerical results

We now discuss some computational aspects and the numerical results, illustrating the feasibility of the real-time resolution of the surface reconstruction problem. Computations are based upon a finite element approximation on \mathbb{P}^1 spaces for the state, control and adjoint variables; the total number of degrees of freedom, i.e. the dimension of the space $\mathcal{Y}_h \times \mathcal{U}_h \times \mathcal{Q}_h$, is $\mathcal{N} = 34818$, obtained using a mesh of 22498 triangular elements. The affine approximation of the parametrized tensors (computed through the empirical interpolation method) entails a parametrized expression of the matrix and vector in (11) made by $Q_k = 53$ and $Q_b = 45$ terms respectively. We have first performed a preliminary test fixing the regularization parameter

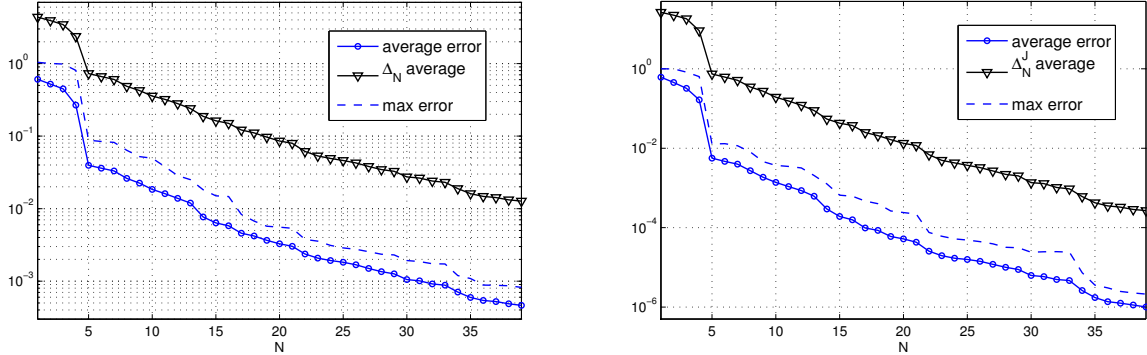


Figure 3: True error and error estimation between the *truth* FE approximation and the RB approximation, for $N = 1, \dots, 39$. On the left true and estimated error on the solution (13), on the right error on the cost functional (16). Regularization parameter $\alpha = 10^{-2}$.

$\alpha = 10^{-2}$: with a fixed tolerance $\varepsilon_{tol}^{RB} = 10^{-2}$ on the a posteriori error bound, $N = 39$ basis functions have been selected by the greedy procedure, thus resulting in a RB linear system of dimension 195×195 . In Figure 3 we compare the a posteriori error bound $\Delta_N(\mu)$ with the true error between the FE solution and the RB solution, and the a posteriori error bound $\Delta_N^J(\mu)$ with the true error on the cost functional. The error estimate decreases at the same

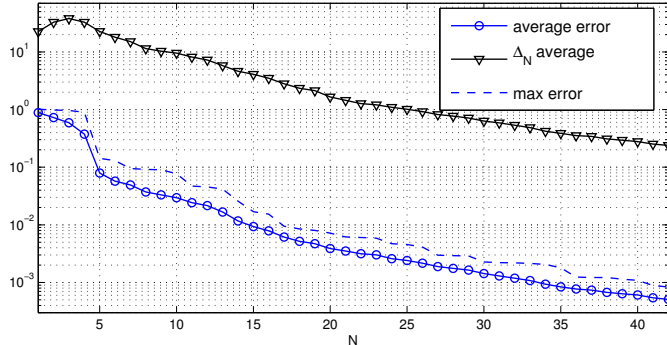


Figure 4: Average computed error and error estimation between the *truth* FE solution and the RB approximation, for $N = 1, \dots, 42$. Regularization parameter $\alpha = 10^{-4}$.

rate of convergence of the true error and it is sharp enough to enable the construction (via the greedy procedure) of a reduced space made by a small number of basis functions. However, independently from the RB approximation, the (relatively high) value used for the regularization parameter results in a poor reconstruction of the unknown surface. For this reason, we have then chosen to use a smaller regularization parameter $\alpha = 10^{-4}$, enabling a more accurate reconstruction of the surface. In this case, while the true error decreases at the same rate as in the previous test, the error estimate shows a lower rate of convergence and becomes less sharp than before, see Figure 4. Therefore, in order to keep a reasonably small number of basis functions, we have decided to stop the greedy procedure after the selection of $N = 42$ basis functions, despite not having reached the desired tolerance; the resulting RB linear system (10) has dimension 210×210 . For this case we report the computational details in Table 1. In Figure 5 some representative examples of reconstructed surfaces obtained through the RB approximation are given; the average time for a single resolution of the optimal control problem is around 0.013 s , while the certification of the solution, i.e. the online evaluation of the a

posteriori error bound⁵, requires around 1 s. As a comparison we report also the time required by the FE solver: the resolution of the optimal control problem without any kind of reduction, nor the shape parametrization neither the affinity approximation, takes more than 30 s, since it requires every time to build the mesh and assemble the FE matrices; exploiting the geometrical reduction and the affinity assumption also for the finite element solver permits to solve the FE approximation in around 1.35 s. Therefore a speed-up of two orders of magnitude is given by the geometrical reduction plus the affinity approximation, while a further speed-up of around two orders of magnitude is given by the computational reduction, i.e. the RB method.

Number of FE dof \mathcal{N}	$3.5 \cdot 10^4$	Linear system size reduction	160:1
Number of parameters P	9	FE full solution t_{FE}^{online} (s)	≥ 30
Number of RB functions N	42	FE affine solution t_{FE}^{online} (s)	1.35
Affine operator components Q_k	53	RB solution t_{RB}^{online} (s)	0.013
Affine rhs components Q_b	45	RB certification t_{Δ}^{online} (s)	0.98

Table 1: Numerical details for the surface reconstruction problem in the case $\alpha = 10^{-4}$. The RB spaces have been built by means of the greedy procedure and $N = 42$ basis functions have been selected. A comparison of the computational times between the online RB evaluations and the corresponding FE simulations is reported.

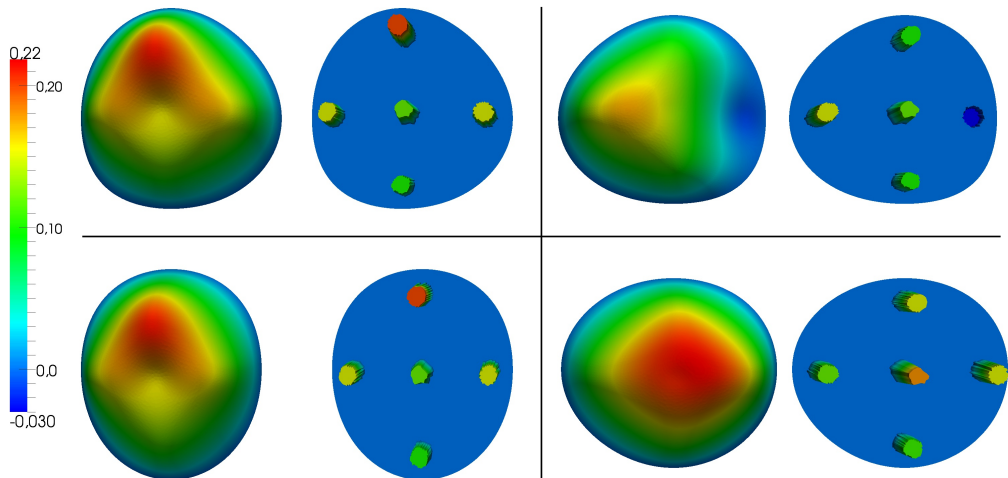


Figure 5: Reconstructed surface y for different geometries and observation values, i.e. different values of the parameters μ . In each box we report the observation values on the right and the reconstructed surface on the left. For instance in the upper boxes the parameters are equal to $\mu = (0.1, 0.1, 0.1, 0.1, 0.15, 0.2, 0.15, 0.1, 0.12)$ on the left and $\mu = (0.15, -0.15, -0.08, 0.03, -0.03, 0.1, 0.15, 0.1, 0.12)$ on the right.

6 APPLICATION TO A BOUNDARY INVERSE PROBLEM

We now consider an inverse boundary problem in hemodynamics, inspired by the recent works [5, 19]. We consider a simplified model of an arterial bifurcation, the parametrized

⁵Note however that the online certification is not strictly necessary as long as the greedy algorithm guarantees that the maximum error over the parameters space is below a desired tolerance.

computational domain (see Figure 6 on the left) features an inflow boundary Γ_{in} , two outflow boundaries Γ_C and the physical wall of the vessel Γ_D . The variables of interest are the velocity \mathbf{v} and the pressure p , supposed to obey the steady Stokes equations (as an approximation of the incompressible Navier-Stokes equations). We suppose to have a measured velocity profile on the red section in Figure 6, but not the Neumann flux on Γ_C that will be our control variable. Starting from the velocity measures we want to find the control variable in order to retrieve the velocity and pressure fields in the whole domain. We consider several possible parameters: geometrical parameters μ_g (e.g. the length of the branches, the angle of the bifurcation etc.), a parametrized (μ_{obs}) measured velocity profile and a parametrized inflow velocity profile $\mathbf{g}(\mu_{in})$. Figure 6 shows the (idealized) *real-time* data assimilation procedure obtainable via the RB method.

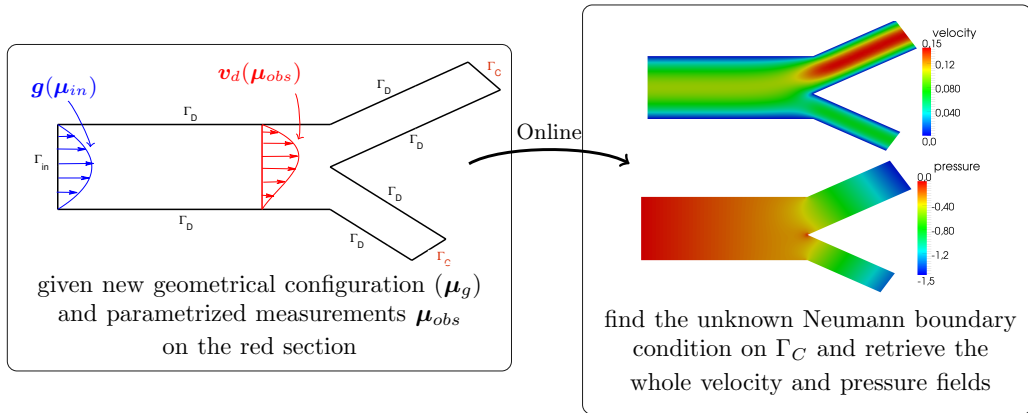
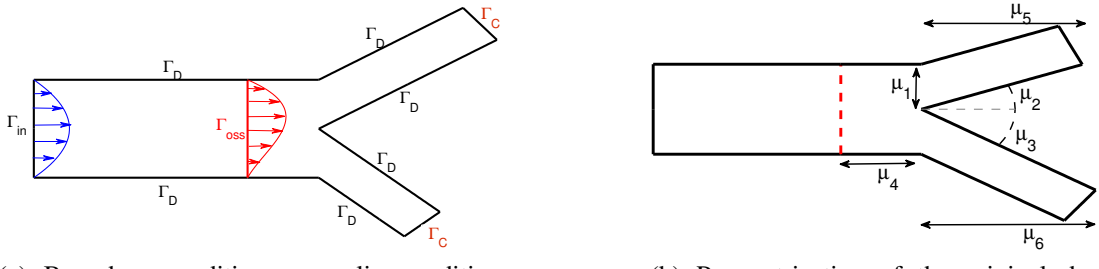


Figure 6: An (idealized) example of inverse boundary problem in haemodynamics. Given a geometrical configuration and some velocity measurements on some sections of the domain, we want to retrieve the whole pressure and velocity fields in order to detect possible pathologies, e.g. occlusions or flow disturbance in arterial bifurcations. Both the geometry and the velocity measurements are obtainable via medical image and data assimilation devices, e.g. MRI; in particular, the velocity profile can be obtained as the output of a smoothing procedure like the one described in the previous section.

The parametrized original domain $\Omega_o(\boldsymbol{\mu})$ is shown in Figure 7: after having fixed the length and the diameter of the large vessel, we have considered six geometrical parameters μ_g representing the height of the upper branch, the angles of the branches with respect to the horizontal line, the length of the two branches and the distance of the observation line Γ_{obs}^o from the bifurcation. The state velocity and pressure variables $\{\mathbf{v}, \pi\}$ satisfy the following Stokes problem in the original domain $\Omega_o(\boldsymbol{\mu})$:

$$\left\{ \begin{array}{ll} -\nu \Delta \mathbf{v} + \nabla \pi = 0 & \text{in } \Omega_o(\boldsymbol{\mu}), \\ \operatorname{div} \mathbf{v} = 0 & \text{in } \Omega_o(\boldsymbol{\mu}), \\ \mathbf{v} = 0 & \text{on } \Gamma_D^o(\boldsymbol{\mu}), \\ \mathbf{v} = \mathbf{g}(\mu_{in}) & \text{on } \Gamma_{in}^o(\boldsymbol{\mu}), \\ -\pi \mathbf{n} + \nu \frac{\partial \mathbf{v}}{\partial \mathbf{n}_o} = \mathbf{u} & \text{on } \Gamma_C^o(\boldsymbol{\mu}), \end{array} \right. \quad (26)$$

where \mathbf{u} is the control variable; the inlet velocity profile $\mathbf{g}(\mu_{in})$ is given by a parametrized Poiseuille parabolic profile while the kinematic viscosity is $\nu = 0.04 \text{ cm}^2 \text{s}^{-1}$. Then we consider



(a) Boundary conditions: no-slip conditions on $\Gamma_D(\mu)$, Poiseuille velocity profile $g(\mu_{in})$ on Γ_{in} , unknown Neumann flux on the outflow sections.

(b) Parametrization of the original domain.

Figure 7: Original domain $\Omega_o(\mu)$ of the arterial bifurcation.

the following (parametrized) cost functional to be minimized:

$$\begin{aligned} \mathcal{J}_o(\mathbf{v}(\mu), \pi(\mu); \mathbf{u}(\mu); \mu) = & \frac{1}{2} \int_{\Gamma_{obs}^o} |\mathbf{v}(\mu) - \mathbf{v}_d(\mu)|^2 d\Gamma_o \\ & + \frac{\alpha_1}{2} \int_{\Gamma_C^o} |\nabla \mathbf{u}(\mu) \mathbf{t}_o|^2 d\Gamma_o + \frac{\alpha_2}{2} \int_{\Gamma_C^o} |\mathbf{u}(\mu)|^2 d\Gamma_o, \end{aligned} \quad (27)$$

being \mathbf{t}_o the tangential unit vector to the boundary Γ_C^o . The first term represents the misfit between the observed velocity profile and that predicted by the Stokes model, while the other contributes are regularization terms: the first one penalizing rapid variations of the control variable along the control boundary, the second one penalizing high values of the control variable; in the following we prefer to penalize rapid variations rather than high values. The observed velocity profile \mathbf{v}_d on Γ_{obs}^o is assumed to be zero in the vertical component, while the horizontal component is assumed to be given by a linear combination of two cubic polynomial functions whose weights are considered as parameters (μ_7 and μ_8). Finally, the parameter domain is given by

$$\mathcal{D} = \{\mu = (\mu_1, \dots, \mu_8) \in \mathbb{R}^8 : \mu_i \in [\mu_{m,i}, \mu_{M,i}] \quad \forall i = 1, \dots, 8, \}$$

where

$$\mu_m = (0.7, \pi/7, \pi/7, 0.7, 1.5, 1.5, 0, 0.5), \quad \mu_M = (1.3, \pi/3, \pi/3, 1.2, 2.5, 2.5, 1, 1.5).$$

In order to formulate the problem as in (17), let us define the appropriate functional spaces for the pressure and velocity variables, $M_o = L^2(\Omega_o)$ and $V_o = [H_{\Gamma_D}^1(\Omega_o)]^2$ respectively, where

$$H_{\Gamma_D}^1(\Omega_o) = \{v \in H^1(\Omega_o) : v|_{\Gamma_D} = 0, v|_{\Gamma_{in}} = 0\}.$$

Then we define the state space $\mathcal{Y}_o = V_o \times M_o$, the adjoint space $\mathcal{Q}_o \equiv Y_o$ and the control space $\mathcal{U}_o = [H^1(\Gamma_C^o)]^2$. In order to recover the formulation (17) we adopt the following correspondences for the trial functions:

$$y = \{\mathbf{v}, \pi\} \in \mathcal{Y}_o, \quad u = \mathbf{u} \in \mathcal{U}_o, \quad p = \{\boldsymbol{\lambda}, \eta\} \in \mathcal{Q}_o,$$

while we denote the test functions of the adjoint space as $q = \{\xi, \tau\} \in \mathcal{Q}_o$. Now let $\mathcal{X}_o = \mathcal{Y}_o \times \mathcal{U}_o$ and $x = (y, u)$, the problem can be formulated as in (17),

$$\min_{x \in \mathcal{X}_o} \mathcal{J}_o(x(\mu); \mu) \quad \text{s.t.} \quad \mathcal{B}_o(x(\mu), q) = \langle G_o(\mu), q \rangle, \quad \forall q \in \mathcal{Q}_o. \quad (28)$$

The bilinear form associated to the state equation is given by

$$\mathcal{B}_o(x, q) = a_o(\mathbf{v}, \boldsymbol{\xi}) + b_o(\boldsymbol{\xi}, \pi) + b_o(\mathbf{v}, \tau) - c_o(\mathbf{u}, \boldsymbol{\xi}) - \langle f_o(\boldsymbol{\mu}), \boldsymbol{\xi} \rangle - \langle g_o(\boldsymbol{\mu}), \tau \rangle.$$

where the bilinear forms $a_o: V_o \times V_o \rightarrow \mathbb{R}$ and $b_o: V_o \times M_o \rightarrow \mathbb{R}$ are those related to the laplacian and divergence operators in the Stokes system, the bilinear form $c_o: U_o \times V_o \rightarrow \mathbb{R}$ is given by

$$c_o(\mathbf{u}, \boldsymbol{\xi}) = \int_{\Gamma_C^o} \mathbf{u} \cdot \boldsymbol{\xi} \, d\Gamma_o,$$

while the linear functional $G_o = \{f_o(\boldsymbol{\mu}), g_o(\boldsymbol{\mu})\}$ is due to the non-homogeneous Dirichlet boundary condition on Γ_{in}^o . Analogously, as already done in the previous section, the cost functional (27) can be expressed in the form (5). Then, we build the affine geometrical mappings as described in Section 4, denoting with $\Omega = \Omega_o(\boldsymbol{\mu}_{ref})$ the reference domain, by choosing (recall that μ_7 and μ_8 are not geometrical parameters)

$$\boldsymbol{\mu}_{ref} = (1, \pi/5, \pi/5, 1, 2, 2, \cdot, \cdot).$$

By tracing problem (28) back to the reference domain we obtain the parametrized formulation (4) and the equivalent saddle-point problem (6), where the affine decompositions (11) holds with $Q_k = 71$ and $Q_b = 20$. The RB approximation described in Section 3 applies with only slightly modifications, mainly due to the enhanced strategy that has to be employed in order to guarantee the stability of the approximation⁶.

6.1 Numerical results

Computations are based upon a finite element approximation on $\mathbb{P}^2 - \mathbb{P}^1$ Taylor-Hood spaces for the velocity and pressure variables, both for the state and adjoint spaces; the total number of degrees of freedom, i.e. the dimension of the space $\mathcal{Y}_h \times \mathcal{U}_h \times \mathcal{Q}_h$, is $\mathcal{N} = 46\,412$, obtained using a mesh of 5 212 triangular elements.

Due to some implementation and computational issues, in this case we avoided to provide the a posteriori error estimation when performing the greedy algorithm: the basis functions have been computed in correspondence of a random set of 65 parameter samples. To check the convergence of the RB approximation we have computed the average error between the *truth* FE solution and the RB approximation, as shown in Figure 8. In Figure 9, 10, 11 we report some representative solutions. For each case we show the geometrical configuration identified by the chosen geometrical parameters as well as the inflow velocity profile and the desired velocity profile on Γ_{obs} depending on the values of μ_7 and μ_8 ; then we show the retrieved velocity and pressure fields. The Online RB evaluation requires less than 0.1s, since we have only to solve the low-dimensional RB linear system (however providing also the a posteriori bound should not require more than a couple of seconds).

7 CONCLUSION

In this work we have presented a reduced framework for the real-time resolution of parametrized PDE-constrained optimization problems, which has been applied to some data reconstruction and data assimilation problems arising in haemodynamics. The RB scheme we have

⁶Since the state problem is weakly coercive itself (rather then strongly coercive as in the previous example) we have to fulfill two nested stability condition: the inner one for the Stokes operator and the outer one for the optimal control problem. The former can be fulfilled by introducing suitable *supremizer operators* [23], while for the latter it suffices to use the aggregated spaces defined in Section 3.

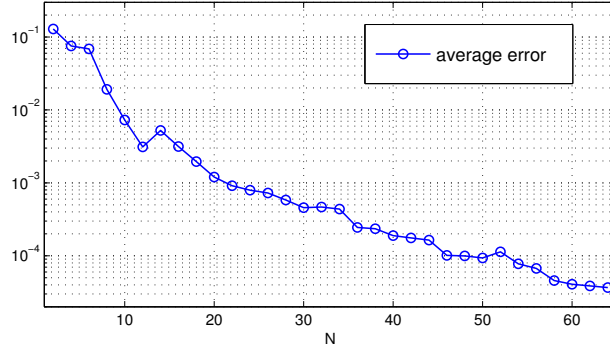


Figure 8: Average computed error between the *truth* FE solution and the RB approximation.

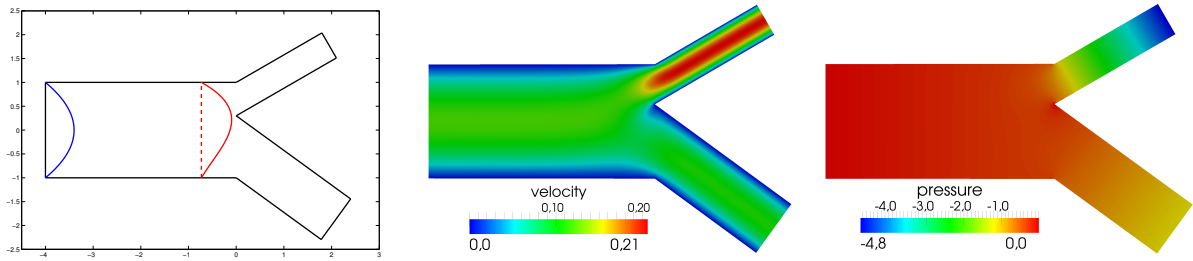


Figure 9: Representative solution for $\mu = (0.7, \pi/6, \pi/5, 0.73, 2.1, 2.4, 0.25, 1.2)$. On the left the input geometrical configuration with plots of the inflow velocity profile and desired velocity profile on Γ_{obs} ; on the right velocity [ms^{-1}] and pressure [Pa] fields.

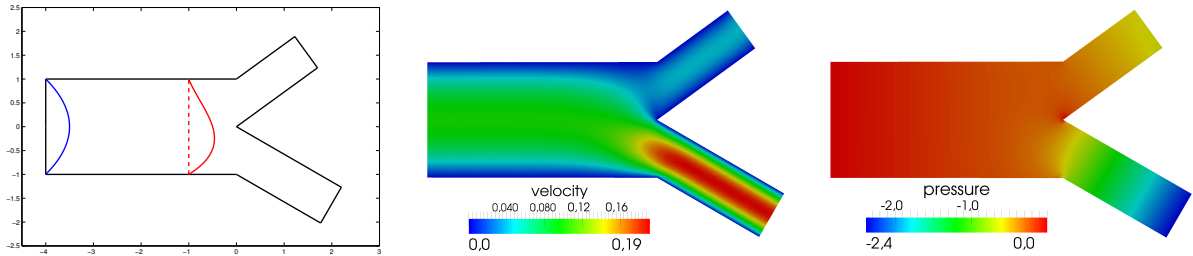


Figure 10: Representative solution for $\mu = (1, \pi/5, \pi/6, 1, 1.7, 2.2, 0.8, 1)$. On the left the input geometrical configuration with plots of the inflow velocity profile and desired velocity profile on Γ_{obs} ; on the right velocity [ms^{-1}] and pressure [Pa] fields.

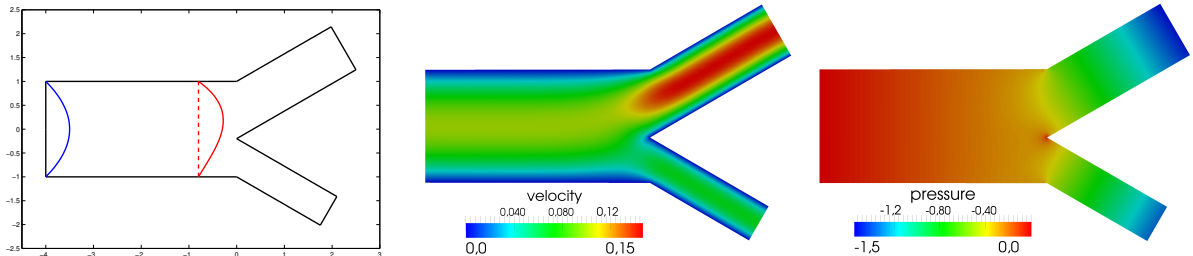


Figure 11: Representative solution for $\mu = (1.2, \pi/6, \pi/6, 0.8, 2.5, 2.1, 0.3, 1)$. On the left the input geometrical configuration with plots of the inflow velocity profile and desired velocity profile on Γ_{obs} ; on the right velocity [ms^{-1}] and pressure [Pa] fields.

proposed is well suited for the general class of parametrized optimal control problems with linear constraint and quadratic functional and it provides the usual features of reduced basis methods; in particular, thanks to the computational strategy employed, the reduced scheme enables the rapid resolution of the optimization problem, as showed in the applications considered.

ACKNOWLEDGEMENTS

We thank Dr. Toni Lassila and Ms. Laura Azzimonti for helpful discussions and valuable feedbacks. We also acknowledge the use of the `rbMIT` package developed by the group of A.T. Patera (MIT) as a basis for the numerical RB simulations.

This work has been supported in part by the Swiss National Science Foundation (Project 141034-122136) and by the ERC-Mathcard Project (Project ERC-2008-AdG 227058).

REFERENCES

- [1] V. Akcelik, G. Biros, O. Ghattas, J. Hill, D. Keyes, and B. Waanders. Parallel Algorithms for PDE-Constrained Optimization. In M.A. Heroux, P. Raghavan, and H.D. Simon, editors, *Parallel Processing for Scientific Computing*, Philadelphia, PA, 2006. SIAM.
- [2] L. Azzimonti, M. Domanin, L. M. Sangalli, and P. Secchi. Surface estimation via spatial spline models with PDE penalization. In *Proceedings of S.Co.2011 Conference*, Padova, 2011.
- [3] F. Brezzi and M. Fortin. *Mixed and Hybrid Finite Elements Methods*. Springer-Verlag, New York, 1991.
- [4] L. Dedé. Reduced basis method and a posteriori error estimation for parametrized linear-quadratic optimal control problems. *SIAM J. Sci. Comput.*, 32:997–1019, 2010.
- [5] M. D’Elia, L. Mirabella, T. Passerini, M. Perego, M. Piccinelli, C. Vergara, and A. Veneziani. Applications of Variational Data Assimilation in Computational Hemodynamics. In D. Ambrosi, A. Quarteroni, and G. Rozza, editors, *Modelling of Physiological Flows*, volume 5 of *MS&A Series*. Springer, 2011.
- [6] M. Grepl and M. Karcher. Reduced basis a posteriori error bounds for parametrized linear-quadratic elliptic optimal control problems. *C. R. Math. Acad. Sci. Paris*, 349(15-16):873 – 877, 2011.
- [7] M. D. Gunzburger. *Perspectives in flow control and optimization*. SIAM, Philadelphia, 2003.
- [8] M. D. Gunzburger and P. B. Bochev. Finite element methods for optimization and control problems for the Stokes equations. *Comp. Math. Appl.*, 48:1035–1057, 2004.
- [9] M. D. Gunzburger and P. B. Bochev. *Least-Squares Finite Element Methods*. Springer, 2009.
- [10] M. Hinze, R. Pinna, M. Ulbrich, and S. Ulbrich. *Optimization with PDE constraints*. Springer, 2009.

- [11] K. Ito and K. Kunisch. *Lagrange Multiplier Approach to Variational Problems and Applications*. Adv. Des. Control. SIAM, 2008.
- [12] K. Ito and S. S. Ravindran. A reduced order method for simulation and control of fluid flows. *J. Comput. Phys.*, 143(2):403–425, 1998.
- [13] J.L. Lions. *Optimal Control of Systems governed by Partial Differential Equations*. Springer-Verlag, Berlin Heidelberg, 1971.
- [14] A. Manzoni. *Reduced models for optimal control, shape optimization and inverse problems in haemodynamics*. PhD thesis, N. 5402, École Polytechnique Fédérale de Lausanne, 2012.
- [15] A. Manzoni, A. Quarteroni, and G. Rozza. Shape optimization for viscous flows by reduced basis method and free form deformation. *Int. J. Numer. Meth. Fluids*, 2011. Available Online.
- [16] A. Manzoni, A. Quarteroni, and G. Rozza. Model reduction techniques for fast blood flow simulation in parametrized geometries. *Int. J. Numer. Meth. Biomed. Engng.*, 28(6-7):604–625, 2012.
- [17] F. Negri. Reduced basis method for parametrized optimal control problems governed by PDEs. Master’s thesis, Politecnico di Milano, Milano, 2011.
- [18] F. Negri, G. Rozza, A. Manzoni, and A. Quarteroni. Reduced basis method for parametrized elliptic optimal control problems. In preparation, 2012.
- [19] M. Perego, A. Veneziani, and C. Vergara. A variational approach for estimating the compliance of the cardiovascular tissue: an inverse fluid-structure interaction problem. *SIAM J. Sci. Comput.*, 33(3):1181–1211, 2011.
- [20] A. Quarteroni, G. Rozza, and A. Manzoni. Certified reduced basis approximation for parametrized PDE and applications. *J. Math in Industry*, 3(1), 2011.
- [21] A. Quarteroni, G. Rozza, and A. Quaini. Reduced basis methods for optimal control of advection-diffusion problems. In *Advances in Numerical Mathematics*, pages 193–216, Moscow, Russia and Houston, USA, 2007.
- [22] T. Ramsay. Spline smoothing over difficult regions. *Journal of the Royal Statistical Society: Series B (Statistical Methodology)*, 64(2):307–319, 2002.
- [23] G. Rozza, D.B.P. Huynh, and A. Manzoni. Reduced basis approximation and a posteriori error estimation for Stokes flows in parametrized geometries: roles of the inf-sup stability constants. Technical Report 22.2010, MATHICSE. Submitted.
- [24] G. Rozza, D.B.P. Huynh, and A.T. Patera. Reduced basis approximation and a posteriori error estimation for affinely parametrized elliptic coercive partial differential equations. *Arch. Comput. Methods Eng.*, 15:229–275, 2008.
- [25] T. Tonn, K. Urban, and S. Volkwein. Comparison of the reduced-basis and POD a-posteriori estimators for an elliptic linear-quadratic optimal control problem. *Math. Comput. Model. Dyn. Syst.*, 17(1):355–369, 2011.

Recent publications :

MATHEMATICS INSTITUTE OF COMPUTATIONAL SCIENCE AND ENGINEERING
Section of Mathematics
Ecole Polytechnique Fédérale
CH-1015 Lausanne

- 13.2012** D. KRESSNER, B. VANDEREYCKEN:
Subspace methods for computing the pseudospectral abscissa and the stability radius
- 14.2012** B. JEURIS, R. VANDEBRIL, B. VANDEREYCKEN:
A survey and comparison of contemporary algorithms for computing the matrix geometric mean
- 15.2012** A. MANZONI, A. QUARTERONI, G. ROZZA:
Computational reduction for parametrized PDEs: strategies and applications
- 16.2012** A.C.I. MALOSSI, J. BONNEMAIN:
Numerical comparison and calibration of geometrical multiscale models for the simulation of arterial flows
- 17.2012** A. ABDULLE, W. E, B. ENGQUIST, E. VANDEN-EIJNDEN:
The heterogeneous multiscale method
- 18.2012** D. KRESSNER, M. PLESINGER, C. TOBLER:
A preconditioned low-rank CG method for parameter-dependent Lyapunov matrix equations
- 19.2012** A. MANZONI, T. LASSILA, A. QUARTERONI, G. ROZZA:
A reduced-order strategy for solving inverse Bayesian shape identification problems in physiological flows
- 20.2012** J. BONNEMAIN, C. MALOSSI, M. LESINIGO, S. DEPARIS, A. QUARTERONI, L. VON SEGESSER:
Numerical simulation of left ventricular assist device implantations: comparing the ascending and the descending aorta cannulations
- 21.2012** A. ABDULLE, M. HUBER:
Discontinuous Galerkin finite element heterogeneous multiscale method for advection-diffusion problems with multiple scales
- 22.2012** R. ANDREEV, C. TOBLER:
Multilevel preconditioning and low rank tensor iteration for space-time simultaneous discretizations of parabolic PDES
- 23.2012** P. CHEN, A. QUARTERONI, G. ROZZA:
Stochastic optimal Robin boundary control problems of advection-dominated elliptic equations
- 24.2012** J. BECK, F. NOBILE, L. TAMELLINI, R. TEMPONE:
Convergence of quasi-optimal stochastic Galerkin methods for a class of PDES with random coefficients
- 25.2012** E. FAOU, F. NOBILE, C. VUILLOT:
Sparse spectral approximations for computing polynomial functionals
- 26.2012** G. ROZZA, A. MANZONI, F. NEGRI:
Reduction strategies for PDE-constrained optimization problems in haemodynamics